2014 5th IEEE RAS & EMBS International Conference on
Biomedical Robotics and Biomechatronics (BioRob)
August 12-15, 2014. São Paulo, Brazil

Detection of Surface Points with an 850nm Laser and an NDI Stereo Camera

Franziska S. Goerlach, Tobias Lueddemann, Jonas Pfeiffer and Tim C. Lueth, *Senior Member, IEEE*

***Abstract*—Accurate three dimensional scanning of surfaces, especially on humans, is more and more relevant. The usage of laser projection systems is widespread. However, a medical certification Class I, high accuracy, a flexible and not static handling as well as the ability to record from more than one direction has never been combined in a single device. Our project aims at the ideal setting for an easy to use, flexible scanning method from more than one recording direction for human tissue without a need of protective equipment. A minimum of requirements for the user and the system itself, as well a possible certification as medical product shall be implemented using a high accurate NDI stereo camera. Interactions and influences of the considered laser modules and reflectors on/with the camera were examined. In this paper, we present, to the authors' best knowledge, novel results of an ideal parameter setting and the requirements based on an 850nm laser module and human tissue for possible applications in navigated surgery or individualized prosthetics.**

Keywords— 3D, 850 nm, contactless, laser scan, NDI Polaris

I. Introduction and Aim

For many applications, e.g. in military, health care, mechanical and manufacturing industry, heritage and archaeology, criminal investigations and the apparel industry, it is desirable to detect the three-dimensional (3D) surface of a geometric body without physical contact [1]–[7]. Two specific applications are particularly important: rapid prototyping [8] and medical technology [9]. In the first case, a main application is reverse engineering [10], [11]. Here, the detected 3D surface of physical objects is imported directly into feature-based CAD systems [12], [13]. In medical technology, further applications are to be found in the areas of individualized limb prosthetics [14], exoskeletons and patient to image registration for navigated surgery systems [15].

The known methods for 3D scans are, in order of their invention: Laser projection [16], stereo images with edge detection [17] and SLAM method (Simultaneous Localization and Mapping) [18], which are comprehensively described in [19] and [9].

For 3D measurement of geometric objects, laser projection methods are primarily used. There are systems from the apparel industry, e.g. from VITRONIC GmbH (Germany, Wiesbaden), that measure the human body to customize garments. For highly accurate 3D scans, e.g. for reverse engineering, rapid prototyping and surface quality control, the systems of Keyence Corporation (Japan, Osaka) and CREAFORM (Canada, Québec), inter alia, are commercially available.

In the application of surgical navigations systems, in practice more than 99% of the used stereo cameras are solely from the manufacturers Northern Digital Inc. (NDI, Canada). These are used for stereoscopic spatial measurements of reflectors with an accuracy of less than 1% [20]. There are also approaches to couple these cameras with laser beam projectors. The Z-Touch laser device (BrainLAB, Germany, Feldkirchen) is a commercially available device, and matches the coordinate system of the surgical field and the 3D patient imaging data using the NDI stereo camera Polaris Spectra.

Based on the applications described above, as well as the restrictions of the solid image format technology (e.g. video cameras), we see the following disadvantages: Current devices for 3D measurement are mainly used for the surface detection of objects, but are not designed for use with humans and/or do not have a high accuracy and/or do not meet the strict legal requirements regarding medical devices. Furthermore, due to their size, these devices are difficult to handle and useable for the most part only stationary and/or with little working distance. Additionally, in most cases only one recording direction is possible, making these devices impractical for a flexible application on humans. Although the mentioned Z-Touch system from BrainLAB is flexible and meets the legal requirements regarding medical devices, it shows an inaccuracy of 2 – 10 mm [21]. Anyway, it is solely for image to patient registration for navigated surgery system and therefore cannot be used for highly accurate 3D measurements.

In summary, there is no flexible, easy to handle, medically approved and commercially available device which allows a highly accurate and contactless 3D laser scan from different recording directions on humans, especially on human faces.

The aim of this work is to realize a hand-held Class I laser device with light points that can be captured with an NDI camera and that can be certified for medical purposes in the future.

This work was supported in part by the Dr. Johannes Heidenhain Foundation (Germany) in 2013.

Franziska S. Goerlach, Tobias Lueddemann, Jonas Pfeiffer and Tim C. Lueth are with the Institute of Micro Technology and Medical Device Technology (MIMED), Technische Universität München, D-85748 Garching, Germany, Phone: +49-89-289-151 59, E-Mail: franziska.goerlach@tum.de).

The challenge is the compromise between the necessary reflection performance on human tissue and the legal requirements (especially safety regarding laser power) for medical products.

The following approach has the potential for an easy to use 3D laser scan for medical applications. The main advantages are scanning from more than one recording direction, a medical certification especially for human faces without protective equipment and high accuracy.

II. Materials and Methods

A. Approach and Structure Description

A schematic of the approach is given in Figure 1: A laser (1) creates a point of light (3) on the object to be measured (2). The laser has a frequency suitable to provide a reflectivity in the visible frequency range of the stereo camera (4). The stereo camera measures the position of the light point in space with two lenses (5). To brighten the scene, the camera features switchable lighting elements (6) in the appropriate frequency range. To enable a synchronization with the lighting elements of the camera, the laser (1) emission can be switched on/off (10) by the control unit (9) via a power transmission path. The control unit receives a signal via a signal transmission path (11) generated by a light sensitive sensor (8). The sensor works in the same frequency as the lighting elements (6) of the camera and is mounted on the object reflector (7) composed of three fixed reflecting balls. Preferably, the sensor (8) is arranged such that the light (6) can only be perceived by the sensor (8) if the object reflector and thus the object to be measured is in the working area of the camera.

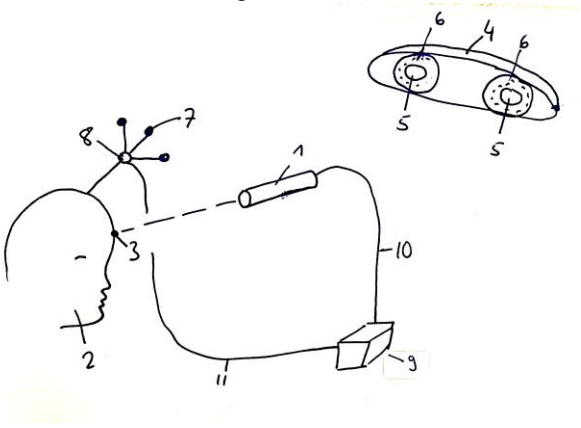

Figure 1. Schematic principle for detecting surface points (3) of an object (2) by a hand-held laser (1) with an NDI stereo camera (4). The laser is triggered by a control unit (9) via a signal transmission path (10) when the light sensitive sensor (8) on the object reflector (7) detects infrared light from the lighting elements (6) of the camera and sends the signal to the control unit via (11). With two lenses (5) the camera is able to calculate the position and orientation of the surface point.

To measure the position of a light point (3) relative to the coordinate system of the object to be measured, the position of the object reflector (7) is measured simultaneously. The position and orientation of the light point and the object reflector are stored separately in homogenous transformation matrices which are sent to a computer unit, not shown in Figure 1.

B. Process Description

With the optical measurement system, the position of the laser beam relative to the object reflector is calculated.

After turning on the control unit (9), the stereo camera (4) begins capturing images for position measurement and returns the position and orientation of all detected reflectors to a computer unit. The stereo camera detects the position of all detectable reflectors with a frequency of 20Hz.

In the following, a short overview of the functioning of the infrared stereo camera and the approach described in Figure 1 is given.

For detecting the reflectors, the camera emits an infrared (IR) light flash, takes a picture sychronously and analyzes it for the brightest reflections spots. As the IR light is mainly reflected by the reflectors and absorbed by the environment, the camera can calculate the position of the reflector relative to the basis coordinate system of the camera. Subsequently, a control picture without flash is taken and compared with the original picture. By this aproach, extraneous light such as sunlight or other IR sources can be excluded as reflectors and discarded. The descriptions of the position and orientation are stored in homogeneous transformation matrices and are sent to the computer unit.

Based on the functioning of the camera described above, a laser beam is synchonized with the camera. A short overview is given for the case when the object to be measured (2) and the object reflector (7)– further referred to as *object* and *reflector*- with the IR light sesitive sensor *IRsensor* (8) are completely in the function range of the camera and not partly covered etc. This process is repeated with a frequency of 20 Hz.

While the internal lighting elements $IRsource_{cam}$ (6) of the camera are switched on, the *IRsensor* (8) measures the incoming IR light. A measurement circuit converts the signal into a corresponding electrical voltage u_{sensor} which is transferred via transmission path (11) to the control unit (9). The control unit detects the voltage and turns on the laser via the transmission path (10) if the voltage exceeds a certain threshold $x_{voltage}$.

Therewith, the condition for the voltage $u_{laser}(t)$ to switch on/off the laser is:

$$u_{laser}(t) = \begin{cases} 1; & u_{sensor} > x_{voltage} \\ 0; & \text{otherwise} \end{cases} \quad (1)$$

The reflection of the laser spot $spot_{laser}$ (3) on the object is recorded during the exposure time t_{cam} by the internal sensors (5) of the camera, as well as the reflection of the IR ratiation from the internal IR lighting elements (6) on the reflector (7).

A control picture $pic_{control}$ is taken by the camera. As no internal IR lighting elements flash, the light sensitive sensor *IRsensor* will not detect any IR light and no electrical voltage u_{sensor} will be transferred to the control unit. Therefore, the laser will not be switched on during the exposure time of the control picture.

To eliminate any extraneous light, the control picture $pic_{control}$ is subtracted from the original picture $pic_{original}$.

Sufficiently bright points will be detected in *pic*.

$$pic = pic_{original} - pic_{control} \quad (2)$$

A sufficiently bright point in *pic* is defined by the camera by a certain amount of pixels meeting the following requirements:
- Each pixel belongs to the 20% brightest pixels in the picture.
- Each pixel's brightness exceeds a camera internal value.

The position and orientation of all detected points will be stored in the coordinate system *cam* of the camera and sent to the computer unit in homogenous transformation matrices **T**.

$$\mathbf{T} = \begin{pmatrix} \mathbf{R} & \mathbf{t} \\ 0 & 1 \end{pmatrix} = \begin{pmatrix} \mathbf{e_x} & \mathbf{e_y} & \mathbf{e_z} & \mathbf{t} \\ 0 & 0 & 0 & 1 \end{pmatrix} \quad (3)$$

R is the rotational part of the matrix which can be separated into the three unit vectors $\mathbf{e_x}$, $\mathbf{e_y}$, $\mathbf{e_z}$. The translational part of the matrix is **t**. Therewith, the exact position and orientation of the reflector *reflector* relative to the camera *cam* or the laser spot $spot_{laser}$ relative to the camera *cam*, is described by

$$^{cam}\mathbf{T}_{reflector} \quad \text{or} \quad ^{cam}\mathbf{T}_{spot_{laser}}. \quad (4)$$

As the static relation between the three reflecting balls of the reflector is known, for the reflector only one homogenous transformation matrix containing the information of the center of the reflector is sent to the computer unit.

We consider the case where the reflector is located in the working area of the camera and is completely visible, i.e. not partly covered. There are two possible scenarios. In the first scenario, the laser spot on the object will be detected by the camera. In the second scenario it will not be detected.

The process on the computer unit is now described for the first scenario where the laser dot will be detected. As the geometry of the reflector is known and the reflector is completely visible, the homogenous transformation matrix of its center $^{cam}\mathbf{T}_{reflector}$ is sent to the computer unit. Additionally, the location of the laser in the coordinate system *cam* is sent in a homogenous transformation matrix $^{cam}\mathbf{T}_{spot_{laser}}$. The location of the laser spot $spot_{laser}$ will be converted into the coordinate system of the reflector *relector* by

$$^{reflector}\mathbf{T}_{spot_{laser}} = \left(^{cam}\mathbf{T}_{reflector}\right)^{-1} \cdot {}^{cam}\mathbf{T}_{spot_{laser}} \quad (5)$$

and will be stored. The data of the reflector will be deleted.

In the second scenario, if the laser spot is not detected (e.g. the reflection was not strong enough or the laser was not aligned to the object), the data of the reflector will be deleted.

Due to the transformation of the coordinate systems described above, the system is especially stable regarding relative motions of the camera and/or the object itself. This allows the flexible use of a hand-held laser and does not demand strict requirements such as a static camera and/or the object to be measured. Freely moving both the measured object and the laser creates a new flexible method of scanning from more than one recording direction. As additionally the precision of the system is exspected to be high due the NDI camera, a new approach of highly accurate scanning without strict requirements to the user is developed.

III. Experiments

In order to find the ideal compromise between the minimal laser spot size and the maximal retro-reflective performance on human skin, various parameters of the above system were examined. For this purpose, the retro-reflective performance of the laser was measured on the back of the hand of three test persons. Therefore, a reproducible measurement setup was constructed.

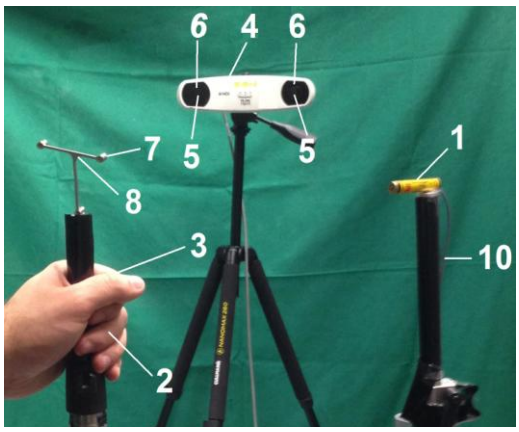

Figure 2. Experiment setting. The laser (1) creates a laser spot (3) on the test person's hand (2). The camera (4) records the scene and calculates the position and orientation of the laser spot (3) and the reflector (7) via two sensors (5). The light sensitive sensor (8) detects the IR light of the camera lighting elements (6) and indirectly triggers the laser by transmission path (10) via a control unit, which is not shown in Figure 2.

The experiments were performed with the laser modules Flexpoint of Lasercomponents (Germany, Olching). The laser modules are focusable, the minimum focus radius of the laser beam was 0.1mm. These laser modules comprise an integrated potentiometer and a separate modulation cable by a maximum output power of 0.01W. All lasers can be triggered with maximum 10kHz. The edge time is specified by the manufacturer to be 200ns. For all settings an, NDI stereo camera Polaris Vicra (type number: P6-00017) was used. It features an internal CCD sensor with corresponding software *NDI Toolbox*. The maximum exploration time of the CCD sensor is 1500µs. The default background sensitivity was set to 1 (1 most sensitive, 7 least sensitive). The distance range of the camera is specified to be between

0.55m to 1.35m. The three reflecting balls of the reflector each have a diameter of 5mm.

A first criterion for the measurement of the retro-reflective performance is fulfilled if the camera detects the laser spot and sends its transformation matrix to the computer unit (further referred to as *measurement 1*). In addition, the NDI Software can download the picture form the CCD Sensor. With an included filter setting, the picture and pixels with sufficient brightness (see definition above) will be colored in red (further referred to as *measurement 2*).

The setting was based on an x-y positioning table. As seen in Figure 2, the camera itself was mounted on a fixed tripod. The laser was mounted on a vertically moveable rod. The test person held a vertically movable rod so that the back of their hand was orientated towards the camera. On top of this rod, the reflector and the light sensitive sensor were mounted. The signal from the sensor was transferred to the control unit. The default distance between the rod and the camera d_{cam} was 1.35m. The default distance between rod and laser d_{laser} was 0.3m. The laser was focused at 0.3m. The data sent from the camera were transferred to a computer unit for further estimations.

Each parameter setting was tested two times separately on three test persons (central European, 20-25 years old) for 90 seconds (i.e. 1800 times).

A. *Influence of Reflector Markers on Exposure Time*

The NDI stereo cameras automatically adapt the internal sensor's exposure time based on the environment. As a preliminary experiment, the influence of reflectors on the exposure time t_{cam} of the camera were examined. The zero-hypothesis $H1_0$ states that the distance of the object reflector has no influence on the exposure time of the camera.

With a step size of 0.1m, the distance between the reflector and the camera was varied. For each step, the exposure time was measured five times.

The results (mean values) are shown in the second column of Table 1. The exposure time t_{cam} increases from ca. 90µs to the maximally possible exposure time t_{max} = 1500µs with increasing distance between the reflector and the camera.

B. *Influence of Different Wavelengths on Spot Detection*

Knowing that the camera has a frequency range in the near infrared range, the ideal wavelength for the maximal retro-reflection on human tissue as detected by the camera had to be examined. The zero-hypothesis $H2_0$ is that the detection of the laser spot is independent of the used laser module, wavelength (ʎ) at any distance d_{cam} from the object to the camera.

The following standard wavelengths in the near infrared range were considered: 780nm, 850nm, 905nm, 940nm, 980nm. Besides the wavelength, all laser modules (further referred to as $laser_1$ to $laser_5$) had the same characteristics above described. With a step size of 0.1m, the object (i.e. without reflector) was set at a distance from the camera. For each step, the exposure time required for the laser spot detection was measured two times separately on the back of the hand of the three test persons. As a measuring criterion, the measurement 1 was chosen. Additionally, a refinement of measurement 1, the exposure time t_{cam} required to detect the laser spot, was recorded.

The results (mean values) are shown in columns 3 to 7 of Table 1. Except the laser spot caused by the $laser_1$ (ʎ = 780nm), all other laser spots were detected in the across the whole distance range of the camera. The mean exposure time $\bar{t}_{cam}$ required for spot detection increases for every wavelength with increasing distance between object and camera. Laser spots of the module with ʎ = 780nm were detected up to a distance of 0.75m (d_{75}) to the camera. For the distances d_{55} to d_{75}, the required $\bar{t}_{cam}$ was t_{max} = 1500µs. For $laser_2$ (ʎ = 850nm) $\bar{t}_{cam}$ increases continuously from 750µs at d_{55} to t_{max} at d_{115} - d_{135}. At d_{55}, $laser_3$ (ʎ = 905nm) generates a $\bar{t}_{cam}$ of ca. 950µs and increases until t_{max} is reached at d_{95} to d_{135}. The value of $\bar{t}_{cam}$at the distance d_{55} of $laser_4$ (ʎ = 940nm) is ca. 1050µs. The maximal exposure time t_{max} is noticed between a distance of 0.85m and 1.35m. The spot of $laser_5$ (ʎ = 985nm) is detected at any distance d_{55} to d_{135} with a required mean exposure time of t_{max} = 1500µs.

TABLE 1: MEAN EXPOSURETIME T_{CAM} OF THE NDI CAMERA IN [µS]

d_{cam} [m]	only object reflector *IRReflector* visible	only $laser_1$ visible ʎ = 780nm	only $laser_2$ visible ʎ = 850nm	only $laser_3$ visible ʎ = 905nm	only $laser_4$ visible ʎ = 940nm	only $laser_5$ visible ʎ = 985nm
0.55	89	1500	750	948	1048	1500
0.65	142	1500	790	1298	1304	1500
0.75	299	1500	830	1468	1435	1500
0.85	494	-	1151	1478	1500	1500
0.95	684	-	1276	1500	1500	1500
1.05	915	-	1372	1500	1500	1500
1.15	1179	-	1500	1500	1500	1500
1.25	1434	-	1500	1500	1500	1500
1.35	1500	-	1500	1500	1500	1500

The mean exposure time $\bar{t}_{cam}$ at distances d_{cam} [m] between the object and the camera were measured for the reflector and five different standard laser modules ($laser_x$) differing in their wavelengths (ʎ = 780nm-980nm). - : the laser spot was not detected.

TABLE 2: DETECTION OF LASER SPOT WITH REFLECTORS IN DISTANCE RANGE OF NDI CAMERA

d_{cam} [m]	$\bar{t}_{cam}$	$laser_1$ ʎ = 780nm	$laser_2$ ʎ = 850nm	$laser_3$ ʎ = 905nm	$laser_4$ ʎ = 940nm	$laser_5$ ʎ = 985nm
0.55	88	-	O	O	O	-
0.65	139	-	X	O	O	-
0.75	305	-	X	X	X	O
0.85	495	-	X	X	X	O
0.95	568	-	X	X	X	O
1.05	913	-	X	X	X	O
1.15	1192	-	X	X	X	X
1.25	1433	-	X	X	X	X
1.35	1500	-	X	X	X	X

-: laser spot not detected by camera. X: laser spot detected by camera (measurement 1 and measurement 2). O: laser spot detected by camera (only measurement 2). $\bar{t}_{cam}$: mean camera exposure time until detection. d_{cam}: distance from the object to the camera in [m].

C. *Interaction of Reflectors and Laser Spots on Detection*

The influence of the reflector on the laser spot detection and vice versa were examined. The first was primarily to examine if the system does detect a laser spot even though a reflector is visible. The latter was to exclude that the laser spot does influence the camera internal detection of reflector markers.

Based on sections A and B, the first zero-hypothesis $H3_0$ is that the laser spot cannot be detected by the camera while the reflector is also visible. The second zero-hypotheses $H4_0$ states that the presence of a laser spot does affect the detection of reflectors.

The setting introduced in section B was modified. The reflector was mounted on top of the rod which the test persons held (Figure 2), such that the reflector and the laser spot were both visible for the camera. As criteria, measurement 1 (M1) and measurement 2 (M2) were considered as well as the mean exposure time $\bar{t}_{cam}$.

The results are shown in Table 2. The camera detects the laser spots of $laser_2$, $laser_3$ and $laser_4$ at any distance, based on M2 and from 0.75m distance according to both criteria M1 and M2. The spots of $laser_1$ were not detected and the spots of $laser_5$ from a distance d_{75} in M2 and from d_{115} in both, M1 and M2.

D. *Influence of Distance Camera – Object on Spot Detection*

As one can derive from the information in Table 1, the greater the distance between the object to be measured and the camera, the smaller the energy of the retro-reflection of the laser on the CCD Sensor. The worst case scenario with respect to retro-reflection performance of laser light on human tissue is to be defined as the greatest possible distance (1.35m) between the object to be measured and the camera.

As seen in Table 2, the retro-reflection performance of $laser_2$ is not strong enough for exposure times smaller than 140µs, with reflectors close to the camera. The worst case scenario with respect to exposure time is 140µs.

E. *Influence of Laser Focus on Spot Detection*

The focus of the laser modules was set to 0.3m. As the system requires a hand-held laser device, the influence of a static focus on the spot detection with respect to the distance from laser to object was examined. The zero hypotheses $H5_0$ states that the focus (thus distance laser-object) does have an influence on the spot detection.

Therefore, an experiment with the same setting as in sectionn C was performed with various distances (0.1m to 1.0m, step size 0.1m) between the laser and the object. The results did not differ at any distance from those presented in Table 2.

F. *Dependency Output Power/Laser ON-Time on Spot Dectection*

To fulfill the strict requirements of medical products, the dependency of output power and laser ON-time was measured. I.e. what duration of laser ON-time is required to detect the laser spot for different output power values?

The setting considered, based on the worst case scenarios, a distance of 1.35m (object-camera). The laser ON-time was triggered by the control unit instead of the *IRsensor*. Figure 3 shows the results for $laser_2$ (λ = 850nm).

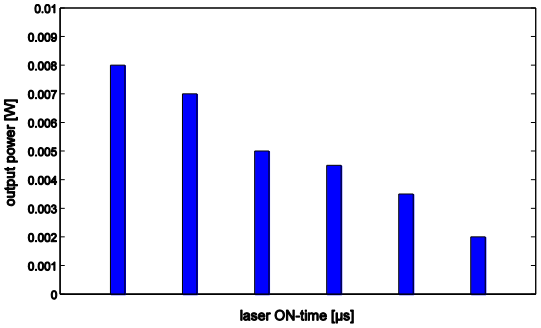

Figure 3. The minimum output power needed in [W] by a fixed laser ON-time in [µs] of an 850nm laser module to detect the laser spot on human tissue with an NDI stereo camera (reflector is visible).

G. *Functionality: Scan of human tissue*

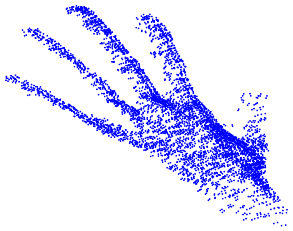

Figure 4. Scan of a test persons hand with 5700 points.

To demonstrate the functionality of the system, Figure 4 displays a scan of the hand of a test person. The scan was performed with an 850nm laser. With a frequency of 20Hz, 5700 points were recorded by an NDI Polaris Vicra.

IV. Discussion and Conclusion

The here made experiments and conclusions were made by the authors to their very best knowledge and examined by them with the greatest possible care. With the chosen boundary conditions, the results are plausible and interpretable.

To fulfill the requirements of this approach and to find the best parameter setting, interaction and influences of the system modules, as well as general questions on the unrestricted functionality had to be answered.

A: To validate the statement that the laser spot does not affect the camera functionality in general and to find the best suiting wavelength, experiments III.A, III.B and III.C were performed.

B: The general possibility to adapt the system, such that it can be certified as medical product, was analyzed in experiment III.F.

C: To prove the functionality in the entire distance range of the camera, experiments III.D, III.E and III.G were accomplished.

Regarding A: As expected, the distance of the object reflector has an influence on the exposure time of the camera. So the zero-hypothesis $H1_0$ must be rejected. If one compares the mean exposure times of experiment III.A with the mean exposure times of experiment III.C, it can easily be seen that the differences between the exposure times caused by reflector and caused by reflector with laser is not significant and based on measurement errors. Although a laser spot is visible in addition to a reflector, the restrictive factor on the exposure time is the reflection of the glass balls of the reflector. I.e. the functionality of the camera is not influenced by laser spots and the zero-hypotheses $H4_0$ has to be rejected, too.

Various wavelengths reflected on human tissue are detected with different intensities by the camera at most distances d_{cam}, i.e. the laser spot detection is dependent on the used laser module at most of the distances between the object and the camera (Table 1), so $H2_0$ has to be rejected. In greater distance to the camera, the different laser modules show the same outcome based on measurement 1 (M1). Considering the refinement of M1, the best results are achieved with laser module $laser_2$ (λ = 850nm), whose spot is detected 250µs (ca. 17%) up to 750µs (ca. 50%) earlier than the spots of the other modules at d_{cam} of 0.55m. Also up to a distance of 1.05m, the required exposure time is at least ca. 10% smaller.

It cannot be differentiated if human tissue reflects various wavelengths in the near infrared range differently or if the camera has an optimal frequency range. Also, it cannot be said, if the surface or deeper layers of tissue were detected.

Even though the mean exposure time $\bar{t}_{cam}$ for the laser modules is higher than the mean exposure time of the reflector (Table 1), a laser spot can be detected (M1) by the camera from a distance of d_{65} on, even if a reflector is visible. Therefore, the zero-hypothesis $H3_0$ from III.C has to be rejected for all laser modules except $laser_1$. The different results based on M1 and M2 cannot be explained. This might be a discrepancy in the software and has to be examined further.

Based on experiment III.B and III.C, we assume $laser_2$ to be the most suitable laser module; $laser_1$ and $laser_5$ can be excluded.

Regarding B: With the results shown in Figure 3, a compromise between laser output power and laser ON-time might be found that fulfills the strict requirements of medical products regarding safety. Hereby, one should consider that the exposure time of the camera due to the reflector at a certain distance is lower than the required ON-time of the laser to be detected. So a compromise has to be found, which may result in a minimum distance (0.75m) for the object to be measured to the camera and further adaption regarding the reduction of the camera frequency (20Hz) to a lower interval, which fulfills the medical standard Class I with the given laser output power/ON-time.

Regarding C: The hypotheses $H5_0$ from III.E has to be rejected, as the spot detection is not affected if the hand-held laser device is held in a distance between 0.1m to 1.0m to the object. Whether the accuracy of the detected location differs through out the different distances, cannot be stated. This has to be examined in further studies.

The fact that the laser spots are not detected at close distances in III.C (Table 2) is caused by the very short exposure time due to the reflector. The energy of the retro-reflection of the laser on the CCD sensors of the camera is not high enough. The spots are not detected as sufficiently bright by definition, which, at this point of time, restrains the system to a minimum distance object to camera of 0.65m. The statement from B restrains the user further to maintain a minimum distance of 0.75m.

In summary it can be said that the approach presented in this paper offers a new flexible 3D scanning method featuring an 850nm laser and an NDI Polaris Vicra. The system has the potential of a possible certification as medical product with minimal handling restrains for the user. The restrains from C affects the user minimally, as the object to be measured should not be too close to the beginning/end of the distance range of the camera anyway to guaranty the visibility of the region of interest for both CCD sensors, i.e. the stereo function.

Applications - after possibly required adaptions - are seen by the authors, inter alia, in surgical navigation, image to patient registration and individualized prosthetics.

ACKNOWLEDGEMENT

This work was supported in part by the Dr. Johannes Heidenhain Foundation (Germany) in 2013.
The authors like to thank in particular Johannes Tenhumberg and Simon Schiele for their excellent support in this project.

REFERENCES

[1] S. Paquette, “3D scanning in apparel design and human engineering,” *IEEE Computer Graphics and Applications*, vol. 16, no. 5, pp. 11–15, 1996.

[2] P. Kühmstedt, C. Bräuer-Burchardt, I. Schmidt, M. Heinze, A. Breitbarth, and G. Notni, “Hand-held 3D sensor for documentation of fossil and archaeological excavations,” in *SPIE Optical Metrology*, 2011, p. 80840U–80840U–8.

[3] R. Marmulla, S. Hassfeld, T. Lüth, and J. Mühling, “Next generation’s navigation systems,” *International Congress Series*, vol. 1256, pp. 467–471, Jun. 2003.

[4] A. Karasik and U. Smilansky, “3D scanning technology as a standard archaeological tool for pottery analysis: practice and theory,” *Journal of Archaeological Science*, vol. 35, no. 5, pp. 1148–1168, May 2008.

[5] W. Schweitzer, E. Röhrich, M. Schaepman, M. J. Thali, and L. Ebert, “Aspects of 3D surface scanner performance for post-mortem skin documentation in forensic medicine using rigid benchmark objects,” *Journal of Forensic Radiology and Imaging*, vol. 1, no. 4, pp. 167–175, Oct. 2013.

[6] S. M. Kim and T. J. Kang, “Garment pattern generation from body scan data,” *Computer-Aided Design*, vol. 35, no. 7, pp. 611–618, Jun. 2003.

[7] R. P. Pargas, N. J. Staples, and J. S. Davis, “Automatic measurement extraction for apparel from a three-dimensional body scan,” *Optics and Lasers in Engineering*, vol. 28, no. 2, pp. 157–172, Sep. 1997.

[8] C. Bradley, G. W. Vickers, and J. Tlusty, “Automated Rapid Prototyping Utilizing Laser Scanning and Free-Form Machining,” *CIRP Annals - Manufacturing Technology*, vol. 41, no. 1, pp. 437–440, Jan. 1992.

[9] I. Gibson, *Advanced Manufacturing Technology for Medical Applications: Reverse Engineering, Software Conversion and Rapid Prototyping (Engineering Research Series (REP))*. Wiley, 2005.

[10] W. B. Thompson, J. C. Owen, H. J. de St. Germain, S. R. Stark, and T. C. Henderson, “Feature-based reverse engineering of mechanical

parts," *IEEE Transactions on Robotics and Automation*, vol. 15, no. 1, pp. 57–66, 1999.
[11] Z. . Xu, S. . Ye, and G. . Fan, "Color 3D reverse engineering," *Journal of Materials Processing Technology*, vol. 129, no. 1–3, pp. 495–499, Oct. 2002.
[12] Y. H. Chen, C. T. Ng, and Y. Z. Wang, "Data reduction in integrated reverse engineering and rapid prototyping," *International Journal of Computer Integrated Manufacturing*, vol. 12, no. 2, pp. 97–103, Jan. 1999.
[13] L. Li, N. Schemenauer, X. Peng, Y. Zeng, and P. Gu, "A reverse engineering system for rapid manufacturing of complex objects," *Robotics and Computer-Integrated Manufacturing*, vol. 18, no. 1, pp. 53–67, Feb. 2002.
[14] D.-J. Yoo and H.-H. Kwon, "Shape reconstruction, shape manipulation, and direct generation of input data from point clouds for rapid prototyping," *International Journal of Precision Engineering and Manufacturing*, vol. 10, no. 1, pp. 103–113, Jul. 2009.
[15] R. Marmulla, T. Lüth, J. Mühling, and S. Hassfeld, "Markerless laser registration in image-guided oral and maxillofacial surgery," *Journal of Oral and Maxillofacial Surgery*, vol. 62, no. 7, pp. 845–851, Jul. 2004.
[16] A. Dipanda and S. Woo, "Towards a real-time 3D shape reconstruction using a structured light system," *Pattern Recognition*, vol. 38, no. 10, pp. 1632–1650, Oct. 2005.
[17] F. Cheng, H. Zhang, D. Yuan, and M. Sun, "Stereo matching by using the global edge constraint," *Neurocomputing*, Nov. 2013.
[18] A. B. Koolwal, F. Barbagli, C. R. Carlson, and D. H. Liang, "A fast slam approach to freehand 3-d ultrasound reconstruction for catheter ablation guidance in the left atrium.," *Ultrasound in medicine & biology*, vol. 37, no. 12, pp. 2037–54, Dec. 2011.
[19] K. Anderson, "Advances in Photogrammetry, Remote Sensing and Spatial Information Sciences: 2008 ISPRS Congress Book , edited by Z. Li, J. Chen, and E. Baltsavias," *International Journal of Geographical Information Science*, vol. 23, no. 5, pp. 685–686, May 2009.
[20] A. D. Wiles, D. G. Thompson, and D. D. Frantz, "Accuracy assessment and interpretation for optical tracking systems," in *Medical Imaging 2004: Visualization, Image-Guided Procedures, and Display*, 2004, vol. 5367, pp. 421–432.
[21] A. Raabe, R. Krishnan, R. Wolff, E. Hermann, M. Zimmermann, and V. Seifert, "Laser surface scanning for patient registration in intracranial image-guided surgery.," *Neurosurgery*, vol. 50, no. 4, pp. 797–801; discussion 802–3, Apr. 2002.